Nerve excitability changes related to muscle weakness in chronic progressive external ophthalmoplegia

Antoine Gueguen,[1] Claude Jardel,[6,2] Marc Polivka,[3] S. Veronica Tan,[4] Françoise Gray,[3] Catherine Vignal,[5] Anne Lombès,[6, 2] Olivier Gout,[1] Hugh Bostock,[4]

[1] Department of Neurology, Fondation Ophtalmologique A. de Rothschild, Paris, France.

[2] Department of Metabolic Biochemistry, AP/HP, Hôpital Pitié-Salpêtrière, Paris, F-75651 France.

[3] Department of Anatomical Pathology, AP/HP, Hôpital Lariboisière, Paris, France.

[4] Institute of Neurology, University College London, London, United Kingdom.

[5] Department of Neuro-Ophthalmology, Fondation Ophtalmologique A. de Rothschild, Paris, France.

[6] INSERM U1016, Institut Cochin, Paris, F-75014 France.

Correspondence to: Hugh Bostock,
Institute of Neurology,
University College London,
Queen Square, London WC1N 3BG, United Kingdom.
E-mail: h.bostock@ucl.ac.uk

Running Title: Nerve dysfunction and weakness in CPEO

Conflict of interest Statement

HB receives royalties from UCL for sales of his Qtrac software used in this study.

Funding

This study received no financial support.

Abstract

Objective: To explore potential spreading to peripheral nerves of the mitochondrial dysfunction in chronic progressive external ophthalmoplegia (CPEO) by assessing axonal excitability.

Methods: CPEO patients (n=13) with large size deletion of mitochondrial DNA and matching healthy controls (n=22) were included in a case-control study. Muscle strength was quantified using MRC sum-score and used to define two groups of patients: CPEO-weak and CPEO-'normal' (normal strength). Nerve excitability properties of median motor axons were assessed with the TROND protocol and changes interpreted with the aid of a model.

Results: Alterations of nerve excitability strongly correlated with scores of muscle strength. CPEO-weak displayed abnormal nerve excitability compared to CPEO-'normal' and healthy controls, with increased superexcitability and responses to hyperpolarizing current. Modelling indicated that the CPEO-weak recordings were best explained by an increase in the 'Barrett-Barrett' conductance across the myelin sheath.

Conclusion: CPEO patients with skeletal weakness presented sub-clinical nerve excitability changes which were not consistent with axonal membrane depolarization, but suggested Schwann cell involvement

Significance: This study provides new insights into the spreading of large size deletion of mitochondrial DNA in CPEO patients.

Highlights

- Patients with chronic progressive external ophthalmoplegia due to large size deletions of mtDNA were studied
- Nerve excitability abnormalities were found that correlated with skeletal muscle weakness
- Abnormalities suggested a spread of mitochondrial dysfunction to Schwann cells

Keywords: CPEO, Mitochondrial disease, Nerve excitability, Myelin sheath, Barrett-Barrett conductance.

Word Count: Abstract: 180; Text: 2425

Introduction

Chronic progressive external ophthalmoplegia (CPEO) is one of the most frequent forms of mitochondrial disease. It may be due to diverse genetic alterations, including mitochondrial DNA (mtDNA) large-size deletion, mtDNA point mutation and alteration of a nuclear gene involved in the mtDNA replication (Dey et al., 2000; Hirano et al., 2001; Holt et al., 1988; Kaukonen et al., 2000; Seneca et al., 2001; Spelbrink et al., 2001; Van Goethem et al., 2001; Zeviani et al., 1989).

In the case of large-size deletions, deleted mtDNA molecules coexist with normal ones (heteroplasmy) and linear correlation has been observed between cellular energy supply and percentage of mutated mtDNA, without a clear threshold above which symptoms appear (Gellerich et al., 2002). The proportion of large-size deletions can differ greatly between different tissues (Shanske et al., 1990), directly influencing the phenotype (Berenberg et al., 1977; Drachman 1968; Shy et al., 1967). The spreading of large-size deletions to the different tissues is not totally understood. It might be related to the time point at which the genetic alteration occurred during embryogenesis: nervous system as well as muscle and other mesoderm tissues would be involved if the alteration occurred before mesoderm and ectoderm differentiation. Mitotic segregation of deleted mtDNA molecules during oocyte maturation could also explain restricted tissue distribution. (Chinnery et al., 2004; Wai et al 2008). Peripheral neuropathy is common in mitochondrial diseases (Filosto et al., 2003; Hirano et al., 2001; Peyronnard et al., 1980; Seneca et al., 2001; Yiannikas et al., 1986). In CPEO it has preferentially been associated with nuclear gene mutations and less classically with large-size deletions. However peripheral nerve functional abnormalities may be overlooked by standard electroneuromyography (ENMG).

The development of computerized threshold-tracking techniques has facilitated non-invasive assessment of the excitability properties of peripheral nerve fibers (Bostock et al.,

1998). These techniques have previously been used to explore the pathophysiology of a wide variety of diseases affecting nerve excitability (Lin et al., 2006; Kiernan & Lin, 2013), including the mitochondrial disease MELAS (mitochondrial myopathy, encephalopathy, lactic acidosis and stroke-like episodes (Farrar et al., 2010). The aim of this study was to use the high sensitivity of nerve excitability measurements to detect spread of mitochondrial dysfunction to peripheral nerve in CPEO.

Materials and Methods

Thirteen CPEO patients with large-size deletions and 22 healthy controls, matching in sex and age, were enrolled in a prospective case-control study. Inclusion criteria were progressive ptosis and ophthalmoplegia, orbital muscle atrophy on MRI or Scan and muscle mitochondrial histologic abnormalities with presence of large-size deletion of mtDNA. The patients were part of the cohort of 69 CPEO patients followed in the neurological department of "Fondation Ophtalmologique A. de Rothschild". The study was approved by the ethical committee of Ile de France VI and conducted in accordance with the provisions of the Declaration of Helsinki. Patients and controls were fully informed of the study modalities and gave their written consent. Medical history was collected in the patients' chart.

Large-size deletion was shown in total DNA extracted from muscle biopsy, using Southern blot and long-range PCR to determine the presence, size and proportion of the deletion. When muscle sample was unavailable for molecular studies, large-size deletion was also looked for in urinary sediment sample using long-range PCR.

MRC sum-score evaluation was performed on eleven groups of muscles (shoulder abductors, elbow flexors and extensors, wrist flexors and extensors, first dorsal interosseous, hip flexors, knee flexors and extensors, foot flexors and extensors) (Kleyweg et al., 1991; Merkies et al., 2003). The MRC sum-score was used to define two groups of CPEO patients:

with normal strength (CPEO-'normal') or with weakness (CPEO-weak). The patients of the latter group presented with skeletal muscle weakness in the four limbs and MRC sum-score <108/110. Slight deltoid weakness was frequent and did not suffice to include in the CPEO-weak patients in the absence of additional muscle weakness.

The multiple measures of nerve excitability were performed on the median motor nerve, once an ENMG procedure had been achieved. The cutaneous temperature was monitored before and after excitability recordings at the stimulation site, to ensure a temperature around 32°C. The stimulating current was applied over the median nerve at the wrist. The anode was placed 10 cm proximally to the cathode over muscle on the lateral part of the forearm. Stimuli were delivered using bipolar constant current stimulator (DS5 stimulator; Digitimer, U.K.). The current intensity was adjusted to reach a CMAP of target amplitude by means of the Qtrac program (written by H. Bostock, copyright Institute of Neurology, UCL, London, UK). CMAP was recorded from the abductor pollicis brevis using a belly-tendon configuration. The signal had 50 Hz noise eliminated with a Humbug (Quest Scientific, Canada) before digitization with a data acquisition card (PCI-6221 National Instruments, U.S.A.) and recording in a computer. Assessment of nerve excitability was performed using the TRONDNF Qtrac recording protocol.

The stimulus-response relationship was established by manually increasing the intensity of stimulation until a CMAP of maximum amplitude was obtained. The program then generated a descending stimulus-response relationship and fitted a curve, which was afterwards used to optimally track a target response set to 40% of the maximal CMAP. Threshold tracking was used to determine the following excitability properties: (i) strength-duration relationship (evaluated as the ‘threshold current’ to reach the target response when the duration of the stimulation decreased from 1 ms to 0.2 ms in 0.2 ms steps); (ii) threshold electrotonus (assessed as the threshold changes during and 100 ms after 100 ms polarizing

currents set to ± 20% and ± 40% of the control threshold); (iii) current/threshold relationship (evaluated as the threshold changes at the end of 200 ms polarizing currents varied from 50% to -100% of the control current threshold in 10% steps); and (iv) recovery cycle (determined as the threshold changes following a supra maximal conditioning pulse at inter-pulse intervals that were gradually decreased from 200 ms to 2 ms). Analysis of the excitability recordings was carried out automatically by the Qtrac software, which generated multiple excitability measurements as described previously (e.g. Table 2 in Tomlinson et al., 2010).

Statistical analysis

Clinical characteristics and excitability parameters were analysed with Fischer test (discrete variables) and Mann-Whitney U-test (continuous variables). Wilcoxon-test was used to analyse repetitive assessments of excitability parameters. Since MRC sum-scores were not normally distributed, they were compared with nerve excitability measurements by Spearman's rank correlation coefficient rho.

The Memfit facility within the QtracP program was used to assess the likely biophysical basis for the abnormal excitability data, by comparison with the 'Bostock' model of nerve excitability (Howells et al., 2012). To fit the model to the real nerve excitability measurements a least squares method was used. For each measurement in the Trond protocol, the discrepancy between the model and the recordings was calculated as: [(xm -xn)/sn] 2, where xm is the threshold of the model, xn the mean and sn the standard deviation of the thresholds for the real nerves. The weights for the measurements within each test were the same but the weights for each test were different (strength-duration relationship = 0.5, threshold electrotonus = 2, current/threshold relationship = 1, recovery cycle = 1).

Results

The characteristics of the two patient groups are compared in Table 1. Nerve excitability did not differ in any of its parameters between the CPEO and control group (Figure 1A-D). Within the CPEO group however threshold changes during polarizing currents (i.e. 'fanning-out' of threshold electrotonus) strongly correlated with muscular weakness, as measured by the MRC sum-score (Figure 2). The greatest correlations were with the responses to hyperpolarizing currents, TEh(10-20 ms) (rho = 0.805), TEh(20-40 ms) (rho = 0.832) and TEh(90-100 ms) (rho = 0.635) .

CPEO-weak patients were thus compared as a group to the CPEO-'normal' and control groups and found to differ with respect to both threshold electrotonus and recovery cycle (Figure 1E-H, Table 2). In response to depolarizing current, reduced threshold was observed during the early stage, ranging from 10 – 20 ms after the beginning of the applied current. From early to late stage, important increase of the threshold was observed during the hyperpolarized current, associated with an abnormal restoration of the threshold after the end of the current. Superexcitability was increased. In contrast, strength duration and current threshold relationship did not differ in any group. CPEO-'normal' and control groups mainly overlapped.

A second evaluation could be performed few months after the initial one in two CPEO-weak patients. In both cases the results of the two evaluations were superimposable, showing very little within-patient variability.

Modelling

To address the biophysical basis of these changes, we used the MEMFIT facility in the QtracP program. Adjustments were made until the discrepancy to the standard model of

human motor axons with the CPEO-'normal' group recordings could not be further reduced. All the model parameters were tested to find which change in the CPEO-'normal' model could best minimize the discrepancy with the CPEO-weak recordings. An increase by 17 % of the conductance of the Barrett and Barrett conductance (GBB) from 36.4 nS (model value) to 42.6 nS reduced the discrepancy between CPEO-weak and CPEO-'normal' by 58.7 % (Figure 3). The GBB parameter represents conduction through the parallel paths across the myelin sheath and around it at the paranode (Barrett et al., 1982). The next best discrepancy reduction was obtained by reducing the nodal and internodal leak conductances (54.5 % and 54.4 % respectively). These changes are physiologically implausible, however, since they involved reducing the conductance by 96.9 % and 99.7 % respectively. We also optimized the fit of the model first to the control group. The best parameter alteration to fit the CPEO-weak patient was an increasing of GBB from 39.3 to 45.3 nS (15.5% increase), which reduced the discrepancy by 65.5%. Modelling of the recording in the most abnormal individual CPEO-weak patient was also best achieved by an increase of GBB, in this case from 36.4 nS to 52.5 nS, which reduced the discrepancy with the CPEO-'normal' patients by 61.5 % (Figure 3).

Discussion

We have found a correlation between muscle strength and nerve excitability in CPEO patients. Abnormal nerve excitability was observed in CPEO patients with skeletal muscle weakness. These changes involved mostly the changes in excitability occurring during and after hyperpolarising currents (i.e. hyperpolarizing threshold electrotonus) as well as the superexcitable period of the recovery cycle. Here we discuss first the likely biophysical basis of the nerve excitability changes, and secondly why they should correlate with weakness.

Biophysical basis of nerve excitability changes

In mitochondrial disease an impaired function of energy-dependent sodium pump (Na+/K+-ATPase) might be expected, which would result in membrane depolarization. Evidence for such an axonal depolarization has been found during stroke like episode in MELAS (Farrar et al., 2010). The effects of ischemic depolarization on nerve excitability are: (i) Threshold Electrotonus 'fanning in' (i.e. smaller threshold changes);. (ii) Current Threshold relationship (IV) similarly shows smaller threshold changes; (iii) In the recovery cycle, the relative refractory period is prolonged, superexcitability is reduced, and subexcitability is reduced to a lesser extent (Kiernan & Bostock, 2000). The pattern of abnormal excitability in CPEO-weak patients was quite different from membrane depolarization, since it included increased superexcitability and increased threshold ('fanning-out') during hyperpolarizing electrotonus

The nerve excitability modelling indicates that GBB increase was the most plausible explanation of the observed abnormalities in the CPEO-weak patients. The GBB was first described by Barrett and Barrett (1982) and is the conductive path between the internodal axolemma and the external medium, which is responsible for the depolarizing afterpotential (DAP), and the resulting superexcitability. GBB comprises conduction across the myelin sheath itself, and also through the imperfect electrical seal between the paranodal loops of myelin and the axolemma. An increase in GBB, whether due to increased leakiness of the myelin or a more leaky paranodal seal, leads to an increase of the DAP and superexcitability, together with an early fanning out of the threshold electrotonus waveforms, as shown in figures 1 and 3. If the increase in GBB were due to a more leaky paranodal seal, one might have expected an increase in nodal fast K conductance due to exposure of some juxtaparanodal K^+ channels. Although a slightly better fit could be obtained by a small

increase in this model parameter, the modelling with two parameter changes is subject to too much uncertainty to be able to draw any conclusions on this question.

The hypothesis of a change in the myelin sheath or paranodal sealing of the myelin is supported by data available from nerve biopsies in mitochondrial myopathies reporting disproportionately thin myelin (Peyronnard et al., 1980) and paracrystalline inclusions in mitochondria of Schwann cells (Yiannikas et al., 1986). Reviewing neuropathies associated with mitochondrial disorders, Schröder (1993) found that the majority of mitochondrial abnormalities were found in Schwann cells rather than axons.

Why does abnormal nerve excitability correlate with weakness?

The correlation between nerve excitability and MRC score is unlikely to be due to any effect of the subclinical nerve dysfunction on muscle, or of muscle weakness on nerve, since the nerve dysfunction was recorded in APB, but weakness was not observed in this muscle in any of the CPEO patients. Moreover, although abnormal nerve excitability may have been present in other nerves, there is no precedent for weakness being caused by such a subclinical nerve abnormality, without evidence of neuropathy on ENMG. In episodic ataxia type 2 (EA2), a very similar subclinical nerve excitability abnormality has recently been reported (Tomlinson et al., 2016), in which an increase in Barrett-Barrett conductance was attributed to nodal malformation in the early neonatal period due to the lack of P/Q calcium channels. Weakness was not evident in those patients (Jen et al., 2001).

Direct involvement of muscle mitochondria is a much more plausible explanation of skeletal muscle weakness in CPEO. We therefore regard it as most likely that the correlation between weakness and nerve excitability changes indicates that the spreading of large-size deletions to ectodermal tissues is associated with heteroplasmy in nerve as well as muscle. The variable spreading of large-size deletion mtDNA would explain the absence of

abnormality in an earlier study with only 4 CPEO patients (Ng et al., 2010). The excitability changes observed in weak patients provide evidence for a spreading of large-size deletions to ectodermal tissue, and consistent with this, CNS involvement with cerebellar ataxia was only seen in patients with nerve excitability abnormalities.

Conclusions

Nerve excitability studies have revealed subclinical axonal changes in a subgroup of large-size deletion CPEO patients with weakness, which suggest a spreading of large-size deletion to Schwann cells, as well as to skeletal muscle, in this more severe phenotype

References

Barrett EF, Barrett JN. Intracellular recording from vertebrate myelinated axons: mechanism of the depolarizing after potential. J Physiol 1982; 323: 117–144.

Berenberg RA, Pellock JM, DiMauro S, Schotland DL, Bonilla E, Eastwood A, et al. Lumping or splitting? "Ophthalmoplegia-plus" or Kearns-Sayre syndrome? Ann Neurol 1977; 1: 37–54.

Bauché S, Boerio D, Davoine CS, Bernard V, Stum M, Bureau C et al. Peripheral nerve hyperexcitability with preterminal nerve and neuromuscular junction remodeling is a hallmark of Schwartz-Jampel syndrome. Neuromuscul Disord. 2013; 23: 998-1009.

Bostock H, Cikurel K, Burke D. Threshold tracking techniques in the study of human peripheral nerve. Muscle Nerve 1998; 21: 137–158.

Chinnery PF, DiMauro S, Shanske S, Schon EA, Zeviani M, Mariotti C et al. Risk of developing a mitochondrial DNA deletion disorder. Lancet 2004; 364: 592–596.

Dey R, Tengan CH, Morita MP, Kiyomoto BH, Moraes CT. A novel myopathy-associated mitochondrial DNA mutation altering the conserved size of the tRNA(Gln) anticodon loop. Neuromuscul Disord 2000; 10: 488–492.

Drachman DA. Ophthalmoplegia plus. The neurodegenerative disorders associated with progressive external ophthalmoplegia. Arch Neurol 1968; 18: 654–674.

Farrar MA, Lin CS, Krishnan AV, Park SB, Andrews PI, Kiernan MC. Acute, reversible axonal energy failure during stroke-like episodes in MELAS. Pediatrics. 2010; 126: 734-739.

Filosto M, Mancuso M, Nishigaki Y, Pancrudo J, Harati Y, Gooch C, et al. Clinical and genetic heterogeneity in progressive external ophthalmoplegia due to mutations in polymerase gamma. Arch Neurol 2003; 60: 1279–1284.

Gellerich FN, Deschauer M, Chen Y, Müller T, Neudecker S, Zierz S. Mitochondrial respiratory rates and activities of respiratory chain complexes correlate linearly with heteroplasmy of deleted mtDNA without threshold and independently of deletion size. Biochim Biophys Acta 2002; 1556: 41–52.

Hirano M, DiMauro S. ANT1, Twinkle, POLG, and TP: new genes open our eyes to ophthalmoplegia. Neurology 2001; 57: 2163–2165.

Holt IJ, Harding AE, Morgan-Hughes JA. Deletions of muscle mitochondrial DNA in patients with mitochondrial myopathies. Nature 1988; 331: 717–719.

Howells J, Trevillion L, Bostock H, Burke D. The voltage dependence of I(h) in human myelinated axons. J Physiol 2012; 590: 1625–1640.

Jen J, Wan J, Graves M, Yu H, Mock AF, Coulin CJ et all . Loss-of-function EA2 mutations are associated with impaired neuromuscular transmission. Neurology 2001; 57:1843-1848.

Kaukonen J, Juselius JK, Tiranti V, Kyttälä A, Zeviani M, Comi GP, et al. Role of adenine nucleotide translocator 1 in mtDNA maintenance. Science 2000; 289: 782–785.

Kiernan MC, Bostock H. Effects of membrane polarization and ischaemia on the excitability properties of human motor axons. Brain 2000; 123: 2542-2551

Kiernan MC, Lin CSY. Nerve excitability: a clinical translation. In: Aminoff MJ, editor. Aminoff's Electrodiagnosis in Clinical Neurology, 6th edn. Amsterdam: Elsevier Saunders; 2012.

Krishnan AV, Kiernan MC. Axonal function and activity-dependent excitability changes in myotonic dystrophy. Muscle Nerve 2006; 33: 627-636.

Kleyweg RP, van der Meché FG, Schmitz PI. Interobserver agreement in the assessment of muscle strength and functional abilities in Guillain-Barré syndrome. Muscle Nerve 1991; 14: 1103–1109.

Lin CS-Y, Kiernan MC, Burke D, Bostock H. Assessment of nerve excitability properties in peripheral nerve disease. In: Kimura J, editor. Clinical Neurophysiology of Peripheral Nerve Disease. Handbook of Clinical Neurophysiology. Amsterdam: Elsevier; 2001. Vol 7, p. 381–403.

Merkies ISJ, Schmitz PIM, Van Der Meché FGA, Van Doorn PA. Comparison between impairment and disability scales in immune-mediated polyneuropathies. Muscle Nerve 2003; 28: 93–100.

Ng K, Winter S, Sue C, Burke D. Preserved motor axonal membrane potential in mitochondrial disease. J Neurol Neurosurg Psychiatr 2010; 81: 844–846.

Peyronnard JM, Charron L, Bellavance A, Marchand L. Neuropathy and mitochondrial myopathy. Ann Neurol 1980; 7: 262–268.

Schröder JM. Neuropathy associated with mitochondrial disorders. Brain Pathol 1993; 3: 177-190.

Shanske S, Moraes CT, Lombes A, Miranda AF, Bonilla E, Lewis E, et al. Widespread tissue distribution of mitochondrial DNA deletions in Kearns-Sayre syndrome. Neurology 1990;40:24-28.

Seneca S, Verhelst H, De Meirleir L, Meire F, Ceuterick-De Groote C, Lissens W, et al. A new mitochondrial point mutation in the transfer RNA(Leu) gene in a patient with a clinical phenotype resembling Kearns-Sayre syndrome. Arch Neurol 2001; 58: 1113–1118.

Shy GM, Silberberg DH, Appel SH, Mishkin MM, Godfrey EH. A generalized disorder of nervous system, skeletal muscle and heart resembling Refsum's disease and Hurler's syndrome. I. Clinical, pathologic and biochemical characteristics. Am J Med 1967; 42: 163–168.

Spelbrink JN, Li FY, Tiranti V, Nikali K, Yuan QP, Tariq M, et al. Human mitochondrial DNA deletions associated with mutations in the gene encoding Twinkle, a phage T7 gene 4-like protein localized in mitochondria. Nat Genet 2001; 28: 223–231.

1 Tomlinson SE, Tan SV, Kullmann DM, Griggs RC, Burke D, Hanna MG, et al. Nerve
2 excitability studies characterize Kv1.1 fast potassium channel dysfunction in patients
3 with episodic ataxia type 1. Brain 2010; 133: 3530–3540.

4 Tomlinson SE, Tan SV, Burke D, Labrum RW, Haworth A, Gibbons VS, et al. In vivo impact
5 of presynaptic calcium channel dysfunction on motor axonal in episodic ataxia type 2.
6 Brain 2016; 139: 380-391.

7 Van Goethem G, Dermaut B, Löfgren A, Martin JJ, Van Broeckhoven C. Mutation of POLG
8 is associated with progressive external ophthalmoplegia characterized by mtDNA
9 deletions. Nat Genet 2001; 28: 211–212.

10 Wai T, Teoli D, Shoubridge EA. The mitochondrial DNA genetic bottleneck results from
11 replication of a subpopulation of genomes. Nat Genet 2008; 40:1484-1488

12 Yiannikas C, McLeod JG, Pollard JD, Baverstock J. Peripheral neuropathy associated with
13 mitochondrial myopathy. Ann Neurol 1986; 20: 249–257.

14 Zeviani M, Servidei S, Gellera C, Bertini E, DiMauro S, DiDonato S. An autosomal dominant
15 disorder with multiple deletions of mitochondrial DNA starting at the D-loop region.
16 Nature 1989; 339: 309–311.

17

Figures

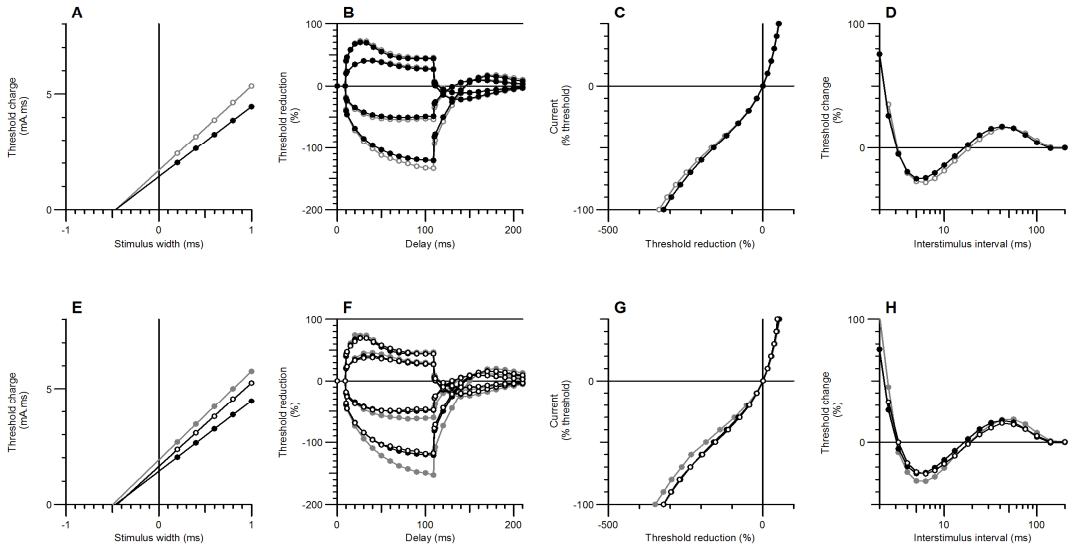

Figure 1.

Figure 1. Comparison of mean nerve excitability waveforms.

Top row (A-D): all CPEO patients (grey empty circles) compared to controls (black filled circles). **Second row (E–H)**: CPEO-weak patients (grey filled circles) compared to CPEO-'normal' (black empty square) and controls (black filled circles). Excitability tests: charge duration relationship (A,E), threshold electrotonus (B,F), current threshold relationship (C,G) and recovery cycle (D,H).

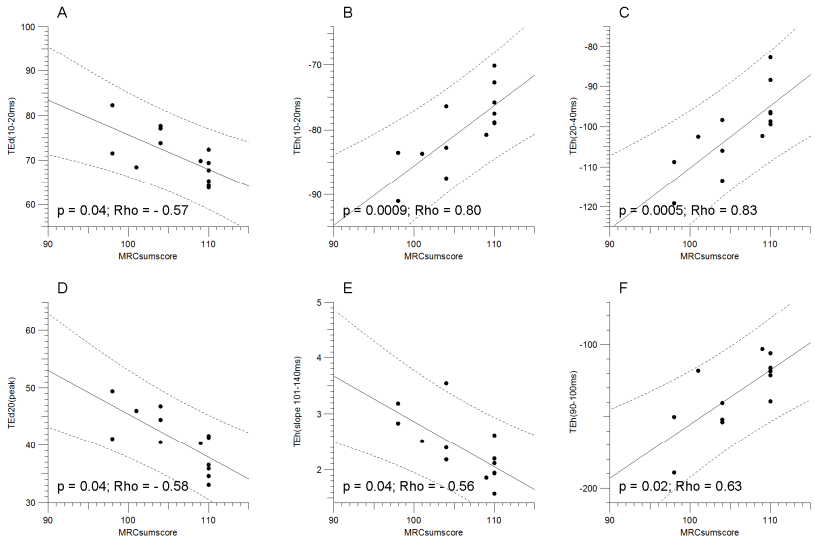

Figure 2.

Figure 2. Correlations between strength (MRC sum-score) and nerve excitability measurements of CPEO patients.

Scatter plots with regression line and 95% confidence limits; **A** – TEd (10-20ms); **B** – TEh (10-20ms); **C** – TEh (20-40ms); **D** – TEd 20 (Peak); **E** – TEh (90-100ms); **F** – TEh (slope 101 – 140ms). Figures show results of Spearman's rank correlation test: p = probability of correlation occurring by change, Rho = correlation coefficient.

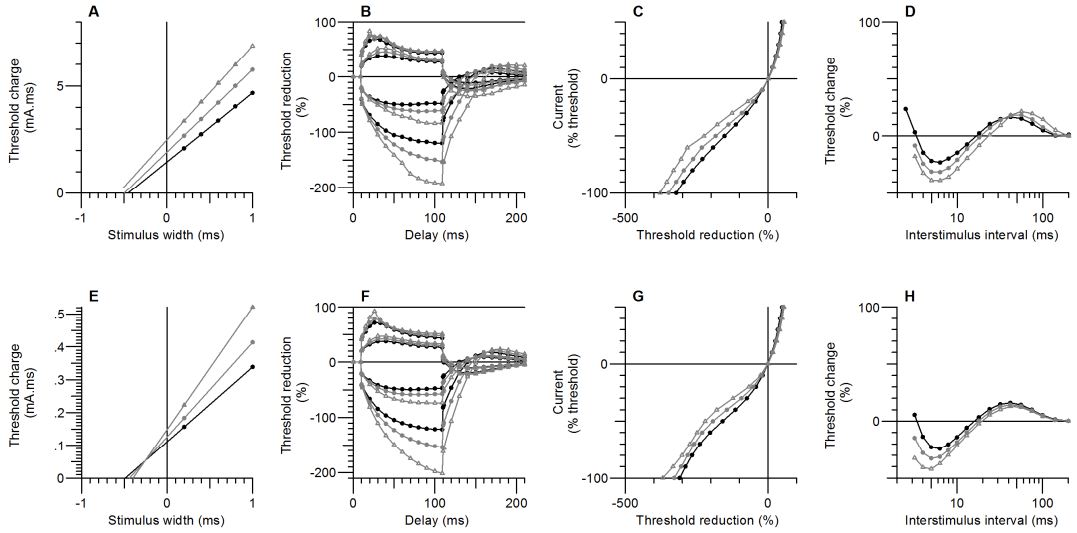

Figure 3.

Figure 3. Modelling of individual and mean nerve excitability waveforms.

Top row (A-D): recorded waveforms: CPEO-'normal' (black filled circles), CPEO-weak (grey filled circles) and the most abnormal CPEO-weak patient (grey filled triangle).

Second row (E-H): modelled waveforms: CPEO-'normal' (GBB=36.4 nS) (black filled circles), CPEO-'normal' modified (GBB=42.6 nS) to fit CPEO-weak (grey filled circles) and CPEO-'normal' modified (GBB=52.5 nS) to fit the most abnormal CPEO-weak patient (grey filled triangle). Excitability tests: charge duration relationship (A,E), threshold electrotonus (B,F), current threshold relationship (C,G) and recovery cycle (D,H).

Table 1. CPEO characteristics

	CPEO-'normal' n = 7	CPEO-weak n = 6	P
Age at onset (years)	19.3 [6– 20]	11.6 [7 – 14]	ns
Sex F/M	3/4	4/2	ns
Ptosis	7	6	ns
Ophthalmoplegia	7	6	ns
Bulbar	1 (14)	4 (66)	0.006
Skeletal UL/LL	1 / 0	6 / 6	-
MRC sum-score	110 [109 – 110]	101 [98 – 104]	-
Heart	2 (28)	1 (16)	ns
Ataxia	0	4 (67)	< 0.0001
Retinopathy	0	0	-
Large size deletion mt DNA	7	6	
Southern blot muscle	7	5	
Long range PCR urine	-	1	-
Size of LSD (Kb)	7 [3 – 8]	6 [4 – 8]	-
mtDNA with LSD (%)	20 [10 – 40]	45 [10 – 50]	-

Data: median [range] or number of patient (percentage); Medical Research Council : MRC; Mitochondrial DNA : mtDNA; skeletal weakness in the upper / lower libs : skeletal UL/LL; PCR : polymerase chain reaction; LSD : large-size deletion; Percentage of mitochondrial DNA with large size deletion : mtDNA with LSD.

Table2. Excitability measurements

	Controls n=22	CPEO n=13	P	CPEO-'normal' n=7	P	CPEO- weak n=6	P	P†
Matching parameters								
Age (years)	57.4 ± 1.4	54.3 ± 2.7	ns	49.4 ± 3.4	0.03	59.8 ± 2.9	ns	ns
Sex (M = 1, F = 2)	1.7 ± 0.1	1.5 ± 0.1	ns	1.3 ± 0.2	ns	1.7 ± 0.2	ns	ns
Temperature (C°)	33.1 ± 0.2	32.8 ± 0.4	ns	33.30± 0.6	ns	32.4 ± 0.4	ns	ns
Stimulus response relationship								
Peak response\(mv)	7.9 ± 1.1	7.6 ± 1.1	ns	8.4 ± 1.1	ns	7.2 ± 1.1	ns	ns
Stimulus-response\slope	4.7 ± 1.1	5.1 ± 1.1	ns	5.1 ± 1.1	ns	4.9 ± 1.1	ns	ns
Stimulus (mA) for 50% max response	4.4 ± 1.1	5.0 ± 1.1	ns	4.9 ± 1.2	ns	5.5 ± 1.2	ns	ns
Strength-duration relationship								
Strength-duration time constant (ms)	0.48 ± 0.0	0.49 ± 0.0	ns	0.48 ± 0.0	ns	0.52 ± 0.0	ns	ns
Rheobase (mA)	2.9 ± 1.1	3.4 ± 1.1	ns	3.4 ± 1.7	ns	3.5 ± 1.2	ns	ns
Threshold Electrotonus								
TEd40(10-20ms)	69.9 ± 0.9	71.0 ± 1.5	ns	67.5 ± 1.2	ns	73.9 ± 1.4	0.03	0.01
TEd40(peak)	68.3 ± 0.9	70.6 ± 1.4	ns	67.6 ± 1.2	ns	73.2 ± 15	0.02	0.02
TEd20(peak)	40.0 ± 0.9	40.9 ± 1.4	ns	37.6 ± 1.3	ns	45.1 ± 1.6	0.02	0.01
TEd40(Accom)	25.1 ± 1.0	25.6 ± 1.1	ns	24.0 ± 1.3	ns	27.07 ± 1.4	ns	ns
TEd(90-100ms)	44.0 ± 1.0	45.4 ± 0.9	ns	43.8 ± 0.7	ns	46.6 ± 1.4	ns	ns
Accommodation half-time (ms)	38.9 ± 0.9	41.9 ± 1.8	ns	45.4 ± 2.1	0.01	38.45 ± 1.8	ns	0.02
TEh40(10-20ms)	-76.7 ± 1.2	-79.9 ± 1.6	ns	-76.4 ± 1.4	ns	-84.2 ± 2.1	0.007	0.01
TEh40(20-40ms)	-95.0 ± 2.0	-101.0 ± 2.7	ns	-95.0 ± 2.6	ns	-108.8 ± 3.7	0.004	0.008
TEh40(90-100ms)	-120.5 ± 4.3	-132.7 ± 6.7	ns	-117.3 ± 4.4	ns	-151.1 ± 9.8	0.004	0.008
TEh40(slope 101-140ms)	2.1 ± 0.1	2.4 ± 0.1	ns	2.0 ± 0.1	ns	2.7 ± 0.2	0.01	0.01
Current/threshold Relationship								
Resting I/V slope	0.59 ± 0.0	0.56 ± 0.0	ns	0.58 ± 0.0	ns	0.53 ± 0.0	ns	ns
Minimum I/V slope	0.24 ± 0.0	0.23 ± 0.0	ns	0.24 ± 0.0	ns	0.21 ± 0.0	ns	ns
Hyperpolarisation I/V slope	0.38 ± 0.0	0.38 ± 0.0	ns	0.40 ± 0.0	ns	0.38 ± 0.0	ns	ns
Recovery cycle								
RRP (ms)	3.0 ± 1.0	3.1 ± 1.0	ns	3.2 ± 1.1	ns	3.0 ± 1.0	ns	ns
Superexcitability (%)	-24.3 ± 1.2	-27.4 ± 1.4	ns	-24.6 ± 1.4	ns	-30.5 ± 2.2	0.02	0.05
Subexcitability (%)	16.6 ± 0.8	16.2 ± 1.7	ns	14.5 ± 2.7	ns	18.25 ± 1.8	ns	Ns

1

CPEO-'normal = CPEO patients with normal strength, CPEO-weak = patients with muscular weakness. Data expressed as mean ± SE; Mann-Whitney U-test are used to compare (i) CPEO, CPEO-'normal' and CPEO-weak to controls : P (ii) CPEO-weak to CPEO;'normal' : P†.

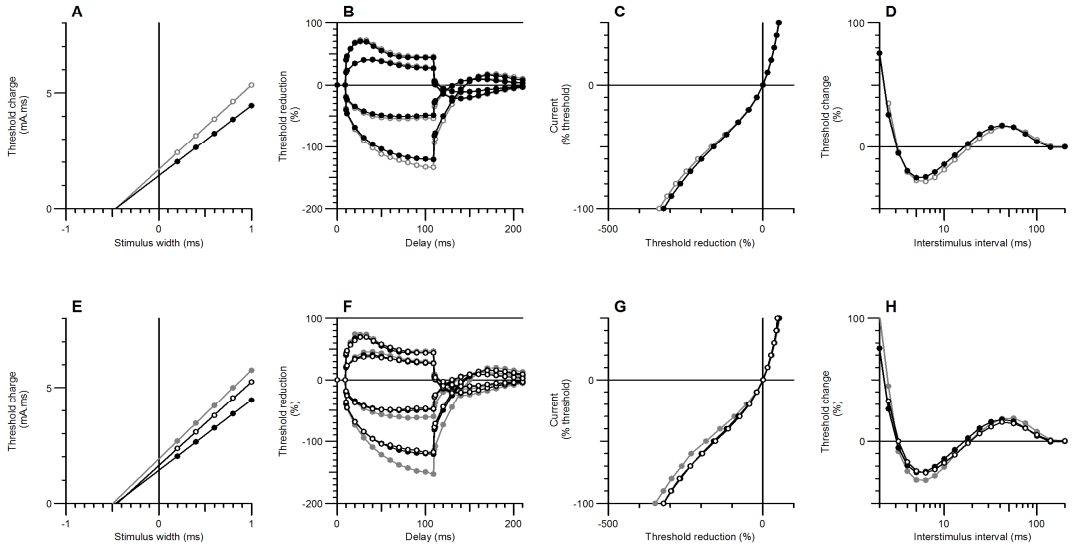

Figure 1.

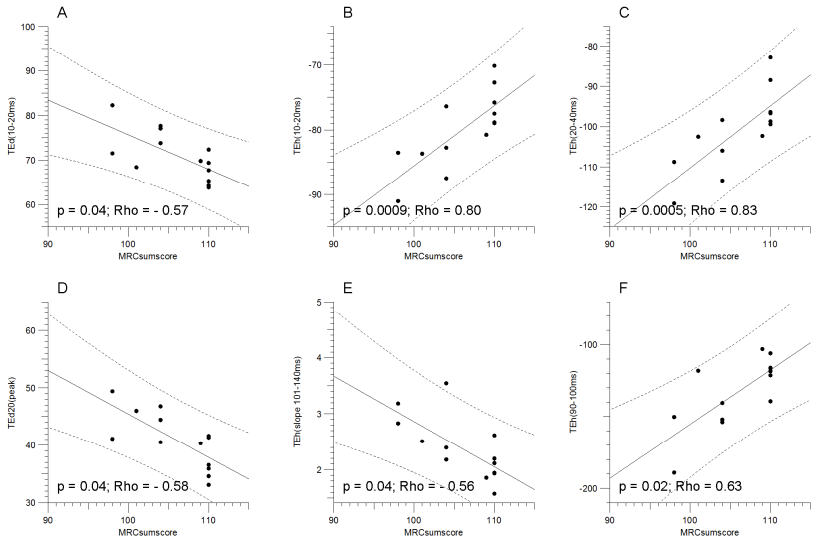

Figure 2.

1

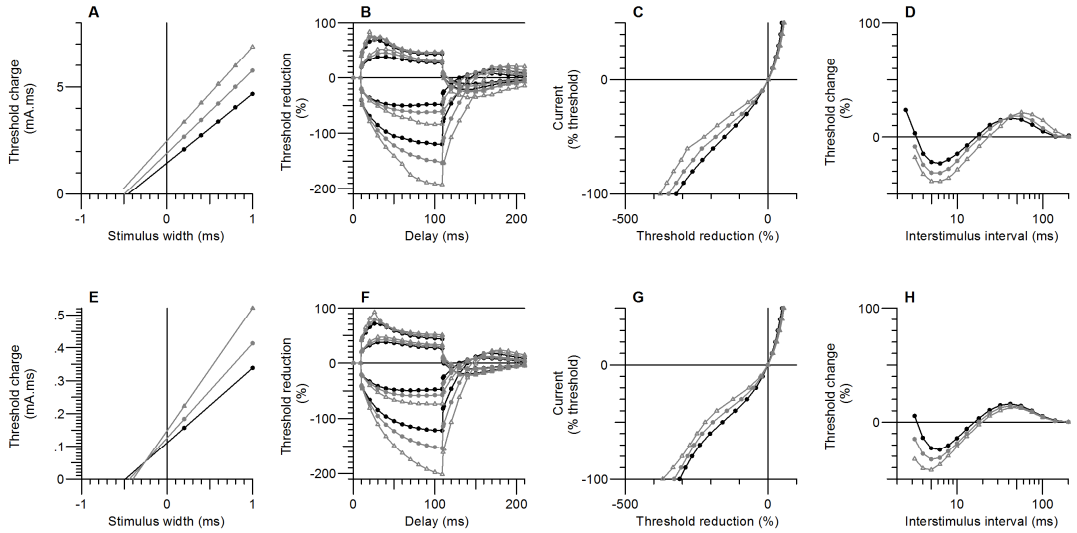

Figure 3.

2